

Performance Analysis of a Multi-Slope Chirp Spread Spectrum Signal for PNT in a LEO Constellation

Daniel Egea-Roca, José López-Salcedo and Gonzalo Seco-Granados
Universitat Autònoma de Barcelona (UAB)
Spain
{daniel.egea,jose.salcedo,gonzalo.seco}@uab.es

Emanuela Falletti
LINKS
Italy
emanuela.falletti@linksfoundation.com

Abstract—During the past few decades, the use of global navigation satellite systems (GNSSs) has become the primary and sometimes only way of providing a positioning, navigation, and timing (PNT) solution for many outdoor applications. Furthermore, GNSS is playing an important role on the development of smart cities and Internet of things (IoT) applications. For this reason, seamless navigation has become very crucial for numerous PNT-dependent applications. Unfortunately, GNSS is a technology that is vulnerable to several threats. All these ingredients boil down to the need for alternative PNT solutions to backup GNSS in case of miss performance or denial of service. The use of low earth orbit (LEO) constellations has been considered in the literature to provide global solution, but more importantly because it will bring some benefits with respect to medium earth orbit (MEO); which is the constellation used in GNSS. Based on these considerations, in this paper we focus on the design of a new PNT signal for LEO constellations. Furthermore, a comprehensive performance analysis is carried out with the aim of reducing the receiver complexity. For that, a chirp spread spectrum signal design is considered.

Index Terms—LEO constellation, Alternative PNT, Chirp Spread Spectrum, GNSS, low-complexity

I. INTRODUCTION

During the past few decades, the presence of global navigation satellite systems (GNSSs) has facilitated positioning, navigation and timing (PNT) for various outdoor applications of our daily life [1]. Furthermore, GNSS is playing an important role in today's smart cities and the futuristic internet-of-things (IoT) [2]. As a matter of fact, seamless navigation has become very crucial for numerous PNT-dependent applications in sensitive fields such as safety and industrial applications. Unfortunately, GNSS signals suffer deterioration due to multipath fading and attenuation in many situations. This is further aggravated by the fact that GNSSs broadcast signals from satellites in medium earth orbit (MEO), resulting in very low received signal power. This makes GNSS vulnerable to intentional and unintentional interference [3]. In this sense, there is a need to think differently about the provision of PNT to critical applications and to consider innovative ways to achieve resilient PNT.

To alleviate these issues, the community trend is to retain GNSS as the backbone PNT but reducing the vulnerabilities of GNSS by using complementary PNT solutions [3], [4]. Among these alternative solutions, multi-sensor fusion technology has become very vital in seamless navigation systems owing to its complementary capabilities to GNSSs [4]. The main drawback of this solution is that they are platform/sensor specific devices, thus limiting the market segment. Other solutions are based on terrestrial radio-frequency signals for which there are mature and commercially available technologies to backup GNSS [3]. However, none of the available solutions can provide a universal backup to GNSS. This is the same for aeronautical radionavigation systems such as VOR, DME and TACAN [5]. Finally, communication signals (e.g., LTE/5G, WiFi, Bluetooth) have been used as signals of opportunity (SoO) for PNT [6]. Nevertheless, they have the same coverage limitation as terrestrial PNT systems. This scene raises the need of a novel complementarity PNT solution that can backup GNSS worldwide any time.

For this end, in the last years, the use of low earth orbit (LEO) satellites for an alternative PNT solution has been investigated [7]. In this sense, one of the key potential aspects to exploit for GNSS complementarity is the space segment represented by LEOs. A proof of that is the extended list of LEO satellite constellations for broadband internet services or IoT connectivity launched in the last few years [8]. For the PNT sector, in contrast to alternative PNT terrestrial solutions, the use of a LEO constellation will give the advantage of providing everywhere connectivity due to the satellite coverage. With respect to MEO constellations, LEO constellations will bring frequency diversity (allowing for interference detection), improvement on the geometry (yielding lower dilution of precision and better performance), and they will provide significantly more powerful signals [9]–[14].

A. LEO PNT system

In this paper, we place the focus on LEO-PNT. A proof of the novelty and scientific interest on LEO-PNT for GNSS complementarity is the publication in Fall 2021 of the first PNT results obtained from the Starlink LEO constellation [9].

This will of course open a new era of alternative PNT solutions based on SoO from LEO constellations, which is confirmed with a similar publication the same year from another research group [12]. Nevertheless, there are still several challenges that need to be solved. The main limitation is the signal design of current LEO constellations, which are mainly designed for communication purposes. This makes GNSS-like measurements from LEO to be inaccurate [11]. This is unfortunate because a proper measurement accuracy would provide a very accurate PNT solution thanks to the fantastic GDOP we find in LEO constellations.

The issue can be solved by transmitting a properly designed PNT signal from the LEO satellites. In other words, we should design an alternative LEO PNT system. This is something that has attracted the commercial interest and today it is a reality by the development of the Xona Space System company [13]. The main drawback of an alternative LEO PNT system is the big infrastructure and effort cost to develop the whole system. One of the most important tasks of such a system is to define the transmitted signal from the satellites, and this will be the focus of this paper. The design of the constellation size, satellite payload and any system design are out of the scope of this paper.

For the signal design, we might adopt the same structure as in GNSS; that is a direct sequence spread spectrum (DSSS) signal. Nevertheless, the acquisition of DSSS signals in LEO constellations may be prohibitive for IoT devices, thus limiting the market segment. The reason is that the high dynamic in LEO constellations will produce a large search space for the acquisition process [14]. One alternative with lower acquisition complexity in LEO can be based on a chirp spread spectrum (CSS) signal. As shown in [14], improvements in terms of complexity from 1 up to 2 orders of magnitude can be obtained using CSS with respect to DSSS.

B. Contribution

Motivated by the reduction of CSS complexity, we will complete the design of the CSS signal in [14] for an alternative LEO PNT solution targeting a complexity optimization. To do so, we first need to analyze the performance of the CSS signal in terms of different figures of merit (FoMs) that have a direct impact on the receiver processing complexity. These FoMs are related with the acquisition sensitivity, the multi-satellite interference (MSI) and the accuracy. These are the main FoMs useful to obtain the ultimate optimization of the complexity. To achieve this target, we provide in this paper a comprehensive analysis of the FoMs of the considered CSS signal. This analysis is done for different simulation parameters involved in the design of a PNT signal such as the signal bandwidth, carrier-to-noise ratio (CN0). Then, based on this parametrical analysis of the CSS signal performance, we provide guidelines for the design of a LEO-PNT signal targeting the optimization of the receiver processing complexity.

Therefore, the contribution of this paper is twofold. First, we provide a comprehensive performance analysis of the CSS signal in terms of FoMs useful for the design of a PNT

signal. Second, we provide signal design guidelines for a low-complexity LEO PNT signal. To do so, the rest of the paper is structured as follows: In Section II we provide the basis for the CSS signal analysis. Next, Section III provides the detailed performance analysis based on the FoMs of a PNT signal. Finally, Section IV concludes the paper by giving a summary of the parametrical performance analysis and providing the guidelines for the CSS signal design targeting the complexity optimization.

II. SIGNAL ANALYSIS SETTING

In this section we introduce the main parameters useful to understand the performance analysis of the CSS signal carried out in this paper. More specifically, we first describe the signal model of the CSS signal studied in this paper. Then, we introduce the study logic followed in this paper to optimize the complexity as well as the definition of the performance metrics to be analyzed.

A. CSS signal model

Chirp spread spectrum (CSS) signals are frequency modulated waveforms that sweep their frequency within the signal bandwidth B during the chirp duration (or period) T_c . In this paper, we consider linear chirps, which are completely characterized by the chirp rate (or slope)

$$\mu \doteq \frac{B}{T_c}. \quad (1)$$

In practice, when considering the presence of both time-delay, τ , and frequency Doppler, f_D , due to propagation, we need the transmission of two chirp components; one with positive slope and another with negative slope [14]. As explained in [14], this is needed for the proper estimation of the pair $\{\tau, f_D\}$, otherwise both parameters are coupled in the chirp frequency and they cannot be separated. This signal structure will be referred as to the BOK-chirp. It is important to note that the data transmission is out of the scope of this paper. We consider that data transmission is obtained with other component or in an additional time-slot as considered in [14].

With the previous setting, we consider the transmission of different BOK-chirp signals from the different satellites in the constellation. So, the following signal is received

$$r(t) = \sum_{i=1}^{N_{\text{vis}}} s_i(t - \tau_i) e^{j2\pi f_D^{(i)}(t - \tau_i)}, \quad (2)$$

where N_{vis} is the number of visible satellites and $\{s_i(t), \tau_i, f_D^{(i)}\}$, with $i = 1, 2, \dots, N_{\text{vis}}$, the transmitted BOK-chirp signal, time-delay and Doppler frequency of the i -th satellite, respectively. For the generation of the different signal waveforms we use the multi-dual slope (MDS) scheme proposed in [14]. This scheme assign two different chirp rates for every satellite in a way that each satellite's signal maintains the same frequency periodicity. To do so, in a constellation with a total of N_{sat} satellites we have:

$$\begin{aligned} \mu_i^{(1)} &= i \frac{2\mu}{N_{\text{sat}}}, \\ \mu_i^{(2)} &= 2\mu - \mu_i^{(1)}, \end{aligned} \quad (3)$$

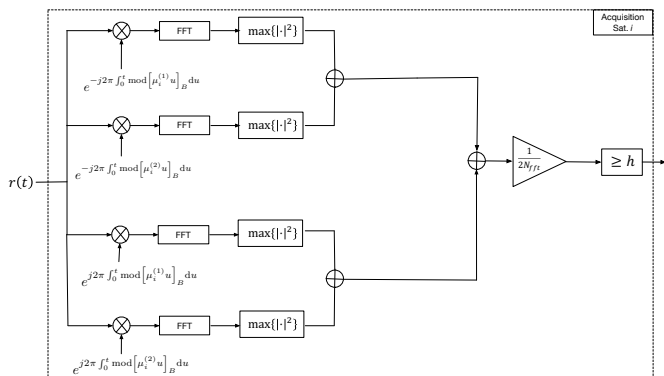


Fig. 1. MDS acquisition block for one channel (i.e., satellite).

with $i = 1, 2, \dots, N_{\text{sat}}$ and the transmitted signal for the i -th satellite given by

$$s_i(t) = \begin{cases} A \cos\left(\pi \text{mod}\left[\mu_i^{(1)} t\right]_B t\right), & t \leq \frac{T_c}{2} \\ A \cos\left(\pi\left(\theta_0 + \text{mod}\left[\mu_i^{(1)} t\right]_B t\right)\right), & \frac{T_c}{2} < t \leq T_c \end{cases}, \quad (4)$$

with $\text{mod}[x]_B$ the modulus B operator of x , $A = \sqrt{2P_s}$, P_s the received signal power, and $\theta_0 = (\mu_i^{(2)} - \mu_i^{(1)})T_c/2$.

The acquisition module for this received signal is shown in Fig. 1. It consists of a total of 4 de-chirp processes, each process composed of a local replica multiplication and further FFT computation. These de-chirps can be divided on the up- and down-chirp branches, which use the negative and positive slopes for the local replica, respectively. Then, each branch has two de-chirps corresponding to the two slopes for each satellite in the MDS scheme. For the signal acquisition, we take the maximum of the (squared absolute value) FFT and we sum the values of the 4 de-chirps together. The result is compared with a threshold to declare the presence or absence of the satellite for which the de-chirp is performed. The block shown in Fig. 1 must be repeated for every satellite in the constellation. The process used to select the detection threshold is based on the definition of the probabilities of detection (PD) and false alarm (PFA). A similar de-chirp-based architecture is applied for parameter estimation as given in [14].

B. Study logic

Let us introduce the study logic for the performance analysis and signal design of the MDS signal. This analysis and design target the minimization of the receiver complexity needed to process the MDS signal. To do so, we would like to have the shortest chirp period possible. Unfortunately, we must fix a large chirp period enough to satisfy different requirements in terms of sensitivity, accuracy or MSI. For this reason, the ultimate chirp period design is driven by the main outcomes of the performance assessment carried out in this paper. The FoMs that will drive our analysis are

- The *sensitivity target*: minimum CN0 needed to obtain $\text{PD} > 0.9$ with $\text{PFA} = 10^{-5}$.
- The level of *MSI*.

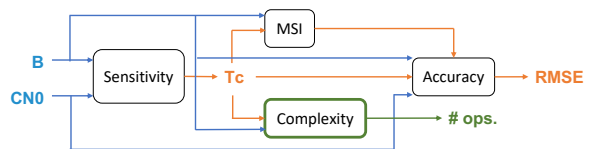


Fig. 2. Study logic followed in the detailed parametrical analysis to be carried out in this paper.

- The *accuracy* of the time-delay and Doppler estimates.
- The signal processing *complexity*.

All these FoMs will be evaluated as a function of different variables such as CN0, time-delay spread, N_{sat} and N_{vis} in a LEO constellation. Figure 2 shows the study logic we will follow for the detailed analysis of the CSS signal.

Since the target design is the complexity, we will look for the minimum chirp period (T_c) that provides the target sensitivity for the given parameters B , CN0, N_{sat} and N_{vis} . Then, with this chirp period and the same parameters, we compute the complexity and the MSI. Once we have the minimum chirp period and its corresponding MSI, we evaluate the accuracy of the given configuration. Before entering into the detailed analysis of the MDS signal following the introduced study logic, let us first give the fundamental definitions needed to understand the analyses carried out in the following sections.

Sensitivity performance

The value of the detection threshold used in the acquisition module of the MDS receiver is configured to provide certain acquisition performance for each satellite. This performance is characterized by the PFA and PD of the acquisition module. In particular, the detection threshold is fixed to provide the sensitivity target performance defined with a $\text{PD} \geq 0.9$ when $\text{PFA} = 10^{-5}$. This is the target sensitivity performance, which of course will be dependent on the signal parameters (i.e., T_c and B) as well as system parameters such as the CN0, N_{sat} and N_{vis} . For the sensitivity analysis to be carried out in Section III, we obtain the value of the detection threshold numerically. This threshold is then used to get the PD we obtain when $\text{PFA} = 10^{-5}$. This process is repeated for every CN0. The PD is also numerically computed with the generation of 10^4 Monte-Carlo realizations of the acquisition process using the previously computed threshold. The computation of the PD is based on the numerical counting of the realizations for which the acquisition variable exceeds the threshold.

Multi-Satellite interference (MSI)

One important aspect in the design of a PNT signal is the multiple access of several satellites. The multiple access for the considered MDS signal is based on the use of different chirp rates for different satellites. The scheme chosen to assign the different chirp rates is intended to build a set of mutually orthogonal chirp-based waveforms. Of course, when the number of satellites increases (with a fixed total bandwidth) the orthogonality between satellites may be compromised, thus leading to a degradation in performance.

To quantify the orthogonality between users, we compute the power excess due to interference between users. To do so,

let us develop the received signal power as

$$P_r = \frac{1}{T_c} \int_0^{T_c} |r(t)|^2 dt = N_{\text{vis}} P_s (1 + \Omega_{\text{MSI}}), \quad (5)$$

in which we have considered equal power for all received signals, given by P_s . The term Ω_{MSI} denotes the normalized power excess due to the interference between BOK-chirps of different satellites. Specifically, we define the MSI as

$$\text{MSI} \doteq \frac{1}{1 + \Omega_{\text{MSI}}} \rightarrow \text{MSI}_{\text{dB}} \doteq -10 \log \left(\frac{P_r}{N_{\text{vis}} P_s} \right). \quad (6)$$

This factor corresponds to a degradation of the CN0, which in turn is translated into a degradation of the MDS signal performance. The analysis of the MSI is useful to fix some limits on the degradation of the accuracy performance due to the interference between satellites.

Ranging accuracy

For the evaluation of the accuracy on the time-delay and Doppler estimates, we base on the root mean squared error (RMSE) of these estimates. For that, we based on the CRLB of a the MDS signal. Without entering into details, based on the definition of the CRLB [15] when considering a sampling rate $F_s = B$, we get the following result for the CRLB of the time-delay estimation of a CSS signal:

$$\text{CRLB}_\tau = \frac{6}{(2\pi)^2 \text{CN0} \cdot B^2 T_c}. \quad (7)$$

It is important to note that this is the CRLB for a BOK-chirp signal. When considering the accuracy of the MDS signal, we have to consider the reception of signals from different satellites. This causes a degradation on the accuracy due to the MSI given by

$$\text{CRLB}_\tau^{(\text{MDS})} = \frac{6}{(2\pi)^2 \text{CN0} \cdot \text{MSI} \cdot B^2 T_c}, \quad (8)$$

with MSI given by (6). Equation (8) will be the cornerstone to bound the accuracy performance of the MDS signal in Section III, and it will be of paramount importance to consolidate the signal design provided in Section IV.

Signal processing complexity

We consider in this paper the complexity of the acquisition process for the MDS signal. The acquisition is composed of 4 de-chirp processes (see Fig. 1), each of them based on a fast Fourier transform (FFT) of the product of the received signal with the local replica. Each FFT is based on a signal of $\tilde{N} = B T_c$ samples. Nevertheless, for a more effective FFT computation we will choose the next power of 2 of \tilde{N} , given by $N = 2^{\text{nextpow2}(\tilde{N})}$.

Doing so, the complexity of the FFT is given by $N \log_2(N)$ [16]. Therefore, summing up, the complexity of the acquisition process for the MDS-based CSS signal is

$$\mathcal{C} \doteq 4N \log_2(N). \quad (9)$$

We will base on this formula in order to compute the number of operations (i.e. complexity) to acquire the CSS signal. For number of operations we consider the number of complex additions followed by a multiplication. We also want to highlight

that this is the complexity needed to acquire 1 satellite with the MDS slope. The same operations have to be repeated for each satellite in the constellation. The previous formula may be useful to get an indication of the level of complexity of the algorithm. We should not take this measure as an exact measure of the complexity, but it is perfect for comparison purposes.

III. PERFORMANCE ANALYSIS

This section reports the results of the parametrical analysis of the considered MDS signal following the study logic shown in Fig. 2. So, in the following sub-sections we show the analysis of the different FoMs considered in this paper, bringing light to consolidated design of the MDS signal.

A. Sensitivity analysis

Let us start with the analysis of the sensitivity performance of the MDS signal. To do so, we analyze the acquisition module shown in Fig. 1 and we perform a parametrical analysis of the sensitivity performance. The main target of this section is to find the minimum chirp period that provides the target sensitivity performance for different values of CN0, N_{sat} and N_{vis} . For the target performance we consider a PD > 0.9 for PFA = 10^{-5} . Then, with this target performance we follow an iterative approach based on the following steps to obtain the minimum chirp period:

- 1) Perform the analysis of the PFA to get the detection threshold that provides PFA = 10^{-5} . The analysis is performed for a randomly chosen satellite.
- 2) Perform the analysis of the PD for the given satellite and random interference. That is, we consider N_{vis} satellites. The same satellite as in *Step 1* is considered as the desired satellite. Then, for each Monte-Carlo run we generate $N_{\text{vis}} - 1$ random satellites considered as interferences. We compute the PD based on the threshold obtained in *Step 1* with 10^4 Monte-Carlo runs.
- 3) If PD < 0.9, increase the chirp period T_c . If PD > 0.95, we decrease T_c . In both cases, return to *Step 1*. Otherwise, we end the iterative process and define the minimum chirp period as the last evaluated T_c (i.e., in the last iteration giving $0.9 < \text{PD} < 0.95$).

This is repeated for all the simulated parameters (i.e., $B, N_{\text{sat}}, N_{\text{vis}}$).

Before entering into details on the results, we would like to highlight that the effect of $\{N_{\text{sat}}, N_{\text{vis}}\}$ on the sensitivity results is negligible in terms of chirp period for the range of CN0 (i.e., [35,50] dB-Hz) and B (i.e., [5,20] MHz) considered in this paper. The reason for these results will become apparent when analyzing the MSI in Section III-B. For this reason, for the following simulations if not stated otherwise we will use $N_{\text{sat}} = 50$ satellites and $N_{\text{vis}} = 5$. Then, we place the focus on the trend of the minimum T_c as a function of the CN0. This is an important analysis since it provides us a way to design the chirp period depending on the target CN0. An example of this analysis is given in Fig. 3 in the range of 35 to 50 dB-Hz and different bandwidths. These values of CN0 are relevant

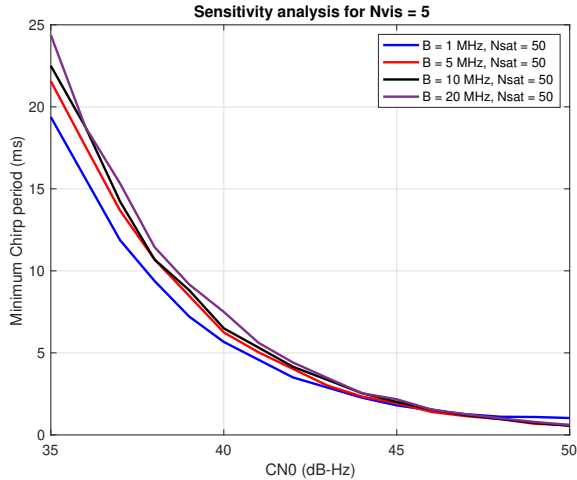


Fig. 3. Minimum chirp period needed to obtain target sensitivity performance ($PD > 0.9$ @ $PFA = 10^{-5}$) for different bandwidths as a function of the CN_0 .

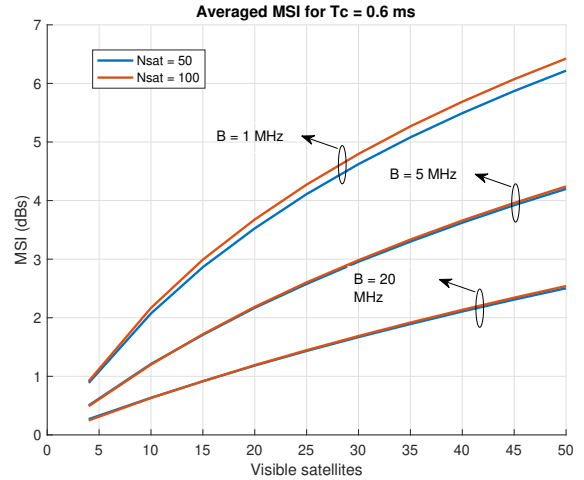


Fig. 4. Multi-Satellite interference of a MDS signal with $T_c = 0.6$ ms as a function of N_{vis} for different bandwidths and N_{sat} values.

for the study of LEO constellations, since their are significant for the path loss experienced in such constellations.

As expected, the highest CN_0 value the shortest chirp period needed to get the target sensitivity performance. Specifically, a chirp period on the order of 20 ms is needed for 35 dB-Hz, but 0.6 ms are enough for 50 dB-Hz. Regarding the bandwidth dependence, we see that for high CN_0 (i.e., 45 – 50 dB-Hz) the minimum chirp period is similar for all the simulated bandwidths in the range of 5 to 20 MHz, but for $B = 1$ MHz the minimum chirp period is larger than for $B > 5$ MHz. On the other hand, for low CN_0 (i.e., 35 – 40 dB-Hz) we get a larger chirp period for larger bandwidths. The reason is related with the number of samples needed to average the noise and allow the proper acquisition. The number of samples in a chirp period is given by the product $T_c \cdot B$. Finally, it is important to note that simulations have been performed for different time-delay and Doppler spread relevant in LEO constellation (see [14]). The results we obtained are the same for different values. So, we conclude that for the given MDS signal design the effect of the time-delay and Doppler spread is negligible for the sensitivity analysis carried out in this paper.

B. MSI analysis

The objective of this section is to quantify the MSI of the MDS signal. To do so, as done for the sensitivity analysis, we consider a constellation size of N_{sat} satellites and we analyze the MSI for a given set of N_{vis} visible satellites. It is expected (and confirmed with the analysis) that the MSI depends on the visible satellites, both on the number of visible satellites, N_{vis} , and the set of visible satellites. For this reason, we will obtain the MUI as defined in (6) for all the satellites in the constellation and for different sets of visible satellites. For the sake of time consumption of the simulations, we considered 100 different and random sets of visible satellites. Then, we get 100 realizations of different MSI values (considering different

sets of visible satellites) for each satellite in the constellation, and we analyze the results.

One of such analyses is the dependence of the MSI with the number of visible satellites, N_{vis} . The results for $N_{vis} \in [2, 50]$ and $N_{sat} = \{50, 100\}$ satellites for different bandwidths values and $T_c = 0.6$ ms are shown in Fig. 4. We see similar values for different N_{sat} values, but it strongly depends on the number of visible satellites. This behaviour is for any simulated T_c (although not shown) and bandwidth, so that we can conclude that the effects of the constellation size, N_{sat} , are negligible in terms of MSI. Indeed, the maximum difference between the MSI value obtained with $N_{sat} = 50$ or $N_{sat} = 100$ is less than 0.2dB. In absolute terms, the maximum MSI value for $N_{vis} < 20$ is around 3.5 dB for 1 MHz, but it can reach up to more than 6 dB for $N_{vis} = 50$. If we increase the bandwidth up to 20 MHz, the MSI values are reduced up to the order of 1 dB for any $N_{vis} < 50$.

Finally, to conclude the analysis of Fig. 4, it is important to note that if N_{vis} is reduced to 5 satellites (i.e., a common number for LEO constellations), the MSI is < 1.5 dB for all the simulated T_c and bandwidth values. These values for the MSI are small values and they are the reason that the variation of the constellation size and visible satellites on the sensitivity analysis (see Section III-A) is negligible. We have to take into account that the only difference on the sensitivity analysis when varying N_{sat} or N_{vis} is the MSI. Since we obtain low MSI values for the simulated parameters, the effects on the sensitivity are negligible. These are good conclusions, but for the design of a PNT signal we have seen that to have an accurate acquisition process, we are not free when fixing T_c for a given bandwidth and CN_0 value (see Fig. 3). Therefore, we are not completely free to choose the number of samples $N = T_c \cdot B$.

Actually, if we want to get the target sensitivity performance, and the minimum chirp period is chosen, the number of samples is fixed to the minimum number of samples needed

to achieve target performance. It is for this reason that we analyze the MSI when considering the minimum chirp period to get sensitivity performance. To do so, we follow the next approach:

- 1) Get the minimum T_c for a given bandwidth and CN0 value, as done in Section III-A,
- 2) Compute the corresponding MSI for given bandwidth and minimum T_c ,
- 3) Analyze the obtained MSI as a function of the given CN0.

This analysis is of paramount importance to bound the MSI values we obtain when designing the chirp period to achieve the target sensitivity performance. It will be also very important for the accuracy analysis to be carried out in Section III-C. A general conclusion for this analysis is that for a given bandwidth, the MSI increases as the CN0 increases (equivalent to decrease the T_c). From these results we obtained that for $N_{\text{vis}} = 5$ the maximum MSI value we get in the simulations is < 0.55 dB for all the considered bandwidths. The minimum value we obtain is around 0.05 dB. For $N_{\text{sat}} = 20$ satellites, we get MSI values < 1.5 dB for all the considered bandwidths in the range of $\text{CN0} \in [31, 50]$ dB-Hz.

The previous quantitative analysis is based on the averaged MSI, but we know that the instantaneous MSI depends on the set of visible satellites. That is, among the N_{sat} possible satellites, we consider one of them as the desired to be acquired, then the rest of visible satellites (i.e., $N_{\text{vis}} - 1$) are selected randomly. To illustrate this dependency, we analyze the minimum, maximum and average values of the MSI among 100 realizations with different (random) set of visible satellites. For this set of satellites, we consider all the satellites in the constellation as the desired one, and then for each of them we obtain the MSI considering $N_{\text{vis}} - 1$ random satellites (avoiding the desired one). Then, we consider the minimum, maximum and average values among realizations (set of satellites) and desired satellites. This allows us to fix some bounds on the MSI values when considering the sensitivity analysis. The result of this analysis when considering $N_{\text{sat}} = 50$ and $N_{\text{vis}} = 5$ satellites is shown in Fig. 5. A bandwidth of 1 and 20 MHz are considered in the upper and lower plots, respectively. The results show a maximum MSI < 1.5 dB for 1 MHz and < 0.6 dB for 20 MHz. Intermediate MSI values can be obtained for different CN0s values, depending on the set of visible satellites.

C. Accuracy analysis

The accuracy analysis considered in this section is based on the CRLB of a single chirp, but considering the corresponding degradation given by the MSI value. Based on the CRLB defined in (8) we consider a maximum, minimum and average accuracy value given by the MSI bounding as described in Section III-B. Furthermore, we consider the corresponding accuracy when fixing the chirp period as the minimum value needed to achieve target sensitivity performance. The results obtained in this section are important to get possible indications on the design of the MDS signal parameters, in particular

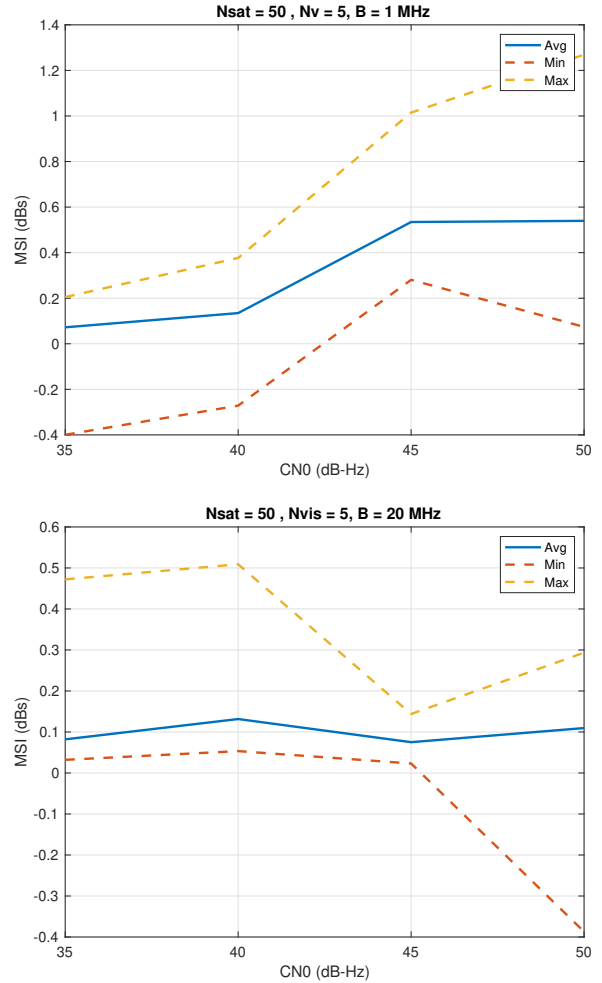


Fig. 5. Multi-Satellite interference bounding when considering sensitivity analysis with $N_{\text{sat}} = 50$ satellites and considering $N_{\text{vis}} = 5$ visible satellites: Minimum, maximum and average values among all satellites in constellation and 100 realizations with different (random) set of visible satellites. (Up) $B = 1$ MHz and (down) $B = 20$ MHz.

for the bandwidth. To obtain these results, we follow again the three-step procedure:

- 1) Get minimum T_c for given bandwidth, B , and CN0t to obtain given sensitivity performance.
- 2) Get MSI for minimum T_c and B . Consider the minimum, maximum and average values.
- 3) Get accuracy given by CRLB in (8) for minimum T_c and B considering $\text{CN0} = \text{CN0t} - \text{MSI}$ (all in dB units). Get minimum, maximum and average values corresponding to the MSI values.

This analysis is a key point to bound the accuracy performance of the MDS signal when designing the chirp period to achieve the target sensitivity performance, and it will be useful for the ultimate design of the signal bandwidth. The results for $N_{\text{sat}} = 50$ and $N_{\text{vis}} = 20$ satellites is shown in Fig. 6 for $B = \{1, 5, 20\}$ MHz. The average and the maximum RMSE values are given considering the average and maximum MSI

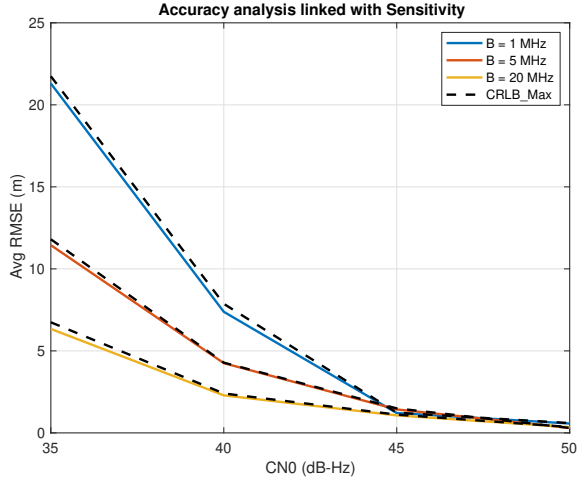


Fig. 6. Accuracy analysis when considering T_c fixed as the minimum value needed to get target sensitivity performance.

values. We see accuracies on the order of tens of meters for $B = 1$ MHz and $CN0 < 40$ dB-Hz, but order of meters can be obtained with the same bandwidth but for $CN0 > 40$ dB-Hz. On the other hand, we get accuracies below 5 m for any $B \geq 5$ MHz and for all $CN0 \geq 40$ dB-Hz. Indeed, we can get below 2 m for $B = 20$ MHz and $CN0 > 40$ dB-Hz. Finally, accuracies below 1 m can be obtained for all simulated $B \geq 1$ MHz and any $CN0 > 45$ dB-Hz. These are useful concluding remarks for a consolidated MDS signal design.

D. Complexity analysis

Finally, let us analyze the MDS receiver complexity based on (9) and the three step procedure followed throughout this section to obtain the minimum T_c needed to achieve the target sensitivity performance. For results showing the dependence of the complexity with the chirp period we refer to [14]. In this section, we consider the constellation altitude and its implications on the MDS signal design. For that, we relate the constellation altitude with the corresponding time-delay span. Then, we consider a T_c equal to this time-delay span, so that an unambiguous time can be measured. Doing so, we can measure the time-delay of any satellite in the constellation unambiguously. That means that the full pseudorange can be measured without needing bit and frame synchronization via the navigation message. That is, we get direct bit synchronization when fixing the chirp period to the time-delay spread of the constellation.

The analysis is based on the comparison of the complexity when fixing $T_c = \tau_{amb}$ and that obtained when fixing $T_c < \tau_{amb}$, with τ_{amb} the time ambiguity. Then, the increment on complexity, ΔC , due to extending the chirp period to $T_c = \tau_{amb}$ to have an unambiguous time measure is derived. We consider two $CN0$ ranges, namely the HIGH and LOW corresponding to [45, 50] and [35, 40] dB-Hz, respectively. Then, we use the chirp periods for HIGH and LOW obtained after the sensitivity analysis (see Section III-A), corresponding

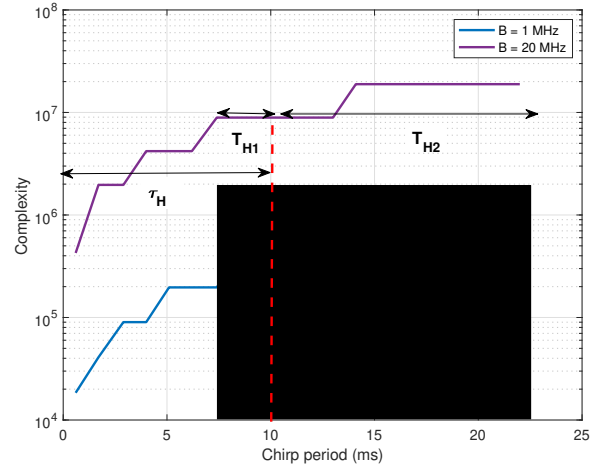
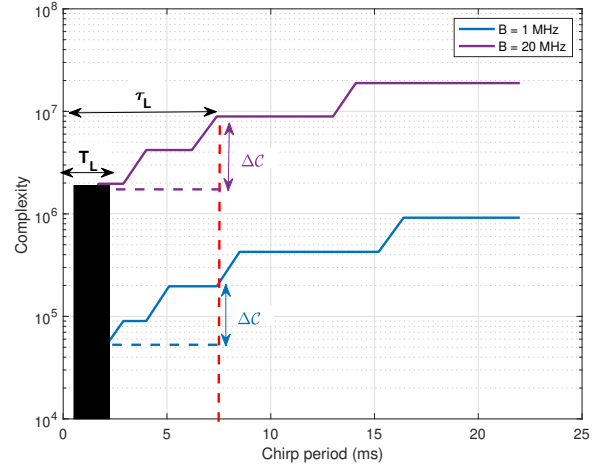


Fig. 7. Complexity analysis as a function of the time-ambiguity for a (Up) HIGH and (Down) LOW $CN0$ regime.

to $T_c \leq T_L = 2.5$ ms and $T_c \geq T_H = 7.5$ ms, respectively. Then, the time ambiguities corresponding to two LEO constellation altitudes are considered. For a low LEO constellation at 600 km of altitude we get $\tau_L = 7.5$ ms and for a high LEO constellation at 1200 km of altitude we get $\tau_H = 10$ ms. Note that we related the HIGH regime with the low LEO constellation and viceversa. The reason is that for a low LEO we consider more received power than a high LEO constellation, due to the difference between propagation losses.

This complexity analysis is shown in Fig. 7. In the upper plot we see how $\tau_L > T_L$, so fixing $T_c = \tau_L$ will provide higher complexity than fixing it to T_L . For instance, @ $B = 20$ MHz we get the complexity for T_L to be $C_L < 2 \cdot 10^6$ and $C_{\tau_L} = 9 \cdot 10^6$. Indeed, we see $\Delta C = C_{\tau_L} - C_L < 4C_L$ for all simulated bandwidths. Therefore, as long as the bit synchronization is not performed in less than 4 timeslots, it is useful to extend the chirp period from T_L to τ_L at the expense of an increment, ΔC , in the complexity. It is important to note that 4 timeslots is equivalent to 4 data communication slots. So, we consider very unlikely to obtain bit synchronization via

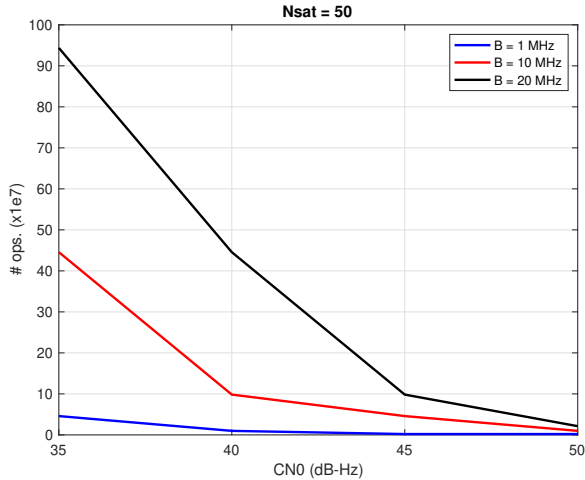


Fig. 8. Complexity analysis as a function of the CN0 (link with sensitivity).

de navigation message in less than 2 data communication slots. Then, the overall complexity to obtain bit synchronization is much smaller when extending the chirp period to be equal to the time ambiguity for a low LEO constellation (i.e., at 600 km). Otherwise, synchronization via frame synch should be performed.

For a high LEO constellation (i.e., at 1200 km), we divide the range of chirp periods in 2 (see lower plot of Fig. 7). The first one considers $T_{H1} \leq \tau_H$, so that if $T_c = \tau_H$ we get unambiguous measure and sensitivity performance. This case is equivalent to the low LEO one and the same conclusions apply. On the other hand, we have the case when $T_{H2} > \tau_H$, so that if $T_c = \tau_H$ we get an unambiguous time measure, but we cannot get the target sensitivity performance. So, as a concluding remark, we see the extension of the chirp period to the time ambiguity useful for the full range of low LEO constellation. For a high LEO it is only useful up to $T_c = \tau_H = 10$ ms and this will provide target sensitivity up to CN0 39 dB-Hz.

Finally, let us analyze the complexity but when considering the chirp period fixed to achieve sensitivity performance. When considering the target sensitivity performance, we cannot freely fix the chirp period for a given B and CN0. So, the complexity cannot be reduced without limits. Indeed, the overall complexity will be driven by the minimum chirp period we need to achieve target performance. Again, we use the following 3-step approach:

- 1) Get minimum T_c needed to achieve target sensitivity performance for given B and CN0 values.
- 2) With the minimum T_c , B and N_{sat} compute the complexity,
- 3) Plot complexity as a function of CN0 for different B values.

This analysis is important to bound the complexity when designing the chirp period to get the target sensitivity performance, and thus it is very useful to optimize a consoli-

dated MDS signal design targeting complexity optimization. An example of this analysis when considering $N_{sat} = 50$ satellites, $B = \{1, 10, 20\}$ MHz and CN0 = [35, 50] dB-Hz is shown in Fig. 8. As expected, the complexity is reduced by increasing the CN0 (or decreasing the chirp period) for a fixed bandwidth. Also, for fixed CN0 (or chirp period), the shorter the bandwidth the lower complexity. Overall, the maximum complexity we get *when only considering 1 satellite channel* is $C \leq 2 \cdot 10^7$ for $B = 20$ MHz @ 35 dB-Hz.

IV. CONCLUSION

Let us conclude the paper by giving a summary of the performance analysis carried out in Section III. Finally, based on this performance analysis, we provide a consolidated MDS signal design for LEO constellations. It is important to note that the target of the analysis and the signal design is the reduction of receiver processing complexity.

A. Summary of performance analysis

We consider the *sensitivity analysis* should be the first analysis to be considered carefully. The reason is that it is the cornerstone for the design of the chirp period, T_c . We have considered the analysis of the minimum T_c needed to achieve the target sensitivity performance: a PD > 0.9 for a PFA = 10^{-5} . Based on this setting and considering LEO constellations with $N_{sat} = [50, 200]$ and $N_{vis} = [5, 20]$ satellites, we obtain a minimum $T_c \sim 20$ ms @ 35 dB-Hz to 0.6 ms @ 50 dB-Hz. Then, once the chirp period is fixed, we have to consider the corresponding *MSI value* for different bandwidth values. As a general conclusion we can say that for the range of simulated parameter values, the MSI value can be considered satisfactory for a PNT signal. The MSI is bounded at 2 dB when considering the minimum T_c . This value is something manageable for a PNT signal in which the accuracy is not the main design target.

For the *accuracy analysis* of the signal, we have considered the CRLB in (8). This allows us to bound the accuracy of the MDS signal when using the minimum T_c . With this framework, and considering $N_{vis} \leq 20$ satellites (an optimistic value for LEO), we identify three levels of accuracy:

- Low accuracy: > 5 m for CN0 < 40 dB-Hz with $B < 5$ MHz.
- Medium accuracy: < 5 m for CN0 ≥ 40 dB-Hz with $B \geq 5$ MHz.
- High accuracy: < 1 m for CN0 ≥ 45 dB-Hz for all $B \geq 1$ MHz.

Finally, once the chirp period and the signal bandwidth are studied, the number of operations needed to process the MDS signal has been evaluated. In base of this analysis and following the study logic considered in this paper a consolidated MDS signal design can be provided. That is, once the minimum chirp period is obtained, an initial consideration of the bandwidth could be taken from the MSI and/or accuracy analysis. Then, with the aim of optimizing the complexity, the final bandwidth value can be tuned according to the results of the *complexity analysis*. As a general conclusion, we get

$2 \cdot 10^4 \leq C \leq 2 \cdot 10^7$ operations (1 satellite channel) for $1 \leq B \leq 20$ MHz and $CN0 \in [35, 50]$ dB-Hz. It is important to remark that these values of complexity are much smaller than the complexity of a DSSS signal in equivalent conditions. Improvements up to 2 orders of magnitudes are shown in [14].

B. Consolidated signal design

Based on the previous summary of the performance analysis, we provide here a consolidated signal design for a LEO constellation. The target is to reduce the receiver processing complexity as much as possible. For this reason, a good use case for the proposed signal design is the IoT use case. For this case, we identify two options when selecting the *chirp period* to optimize the complexity. These options depend on the requirements in terms of sensitivity, complexity and data rate of the use case:

- When data rate and complexity is a requirement with more priority than sensitivity, we should target the shortest chirp period possible. This is done in terms of the target in terms of CN0 (e.g., 40 dB-Hz). Then, we fix the chirp period as the minimum needed to get sensitivity performance at such CN0 (e.g., $T_c \sim 7.5$ ms, depends on bandwidth). This could be a case in which the IoT device is not connected and it needs a relatively high data rate to demodulate data information (e.g., ephemeris).
- When data rate is not a priority, we have freedom on fixing the value of T_c . Here we can fix it as the time-delay span needed to obtain an unambiguous measure. This would allow to have direct bit synchronization, with all the benefits that can bring this in terms of complexity and time to first fix (TTFF) reduction (e.g., no need for bit synchro). For instance, $T_c = 12$ ms provides unambiguous measure up to a high LEO (i.e., at 1200 km) with sensitivity performance @38 dB-Hz. This could be a case in which the IoT device is connected and it can externally download data information.

For the configuration of the *signal bandwidth*, we also have different options. Considering the main target is the optimization of the complexity, we consider a bandwidth in the range of 1 to 5 MHz. This is also coherent with the bandwidths used in practice for the IoT use case. Two possibilities may be to consider the data rate or accuracy to tune the signal bandwidth depending on the specific requirements of the use case:

- Data rate: Considering $T_c = 7.5$ ms and a LoRa-like signal [17] for the data transmission, we have a data rate given by

$$R_b \doteq \frac{BT_c}{T_c}, \quad (10)$$

so that $R_b = \{1.72, 2.02\}$ kbps for $B = \{1, 5\}$ MHz, respectively.

- Accuracy: Considering a chirp period given by the minimum T_c or greater, we have an accuracy $< \{7, 2\}$ m @40 dB-Hz for $B = \{1, 5\}$ MHz, respectively.

Finally, based on these considerations for the chirp period and signal bandwidth of the MDS signal, the corresponding optimized complexity is:

- For $T_c = 7.5$ ms (unconnected device) $C \sim 2 \cdot \{10^5, 10^6\}$ for $B = \{1, 5\}$ MHz, respectively.
- For $T_c = 12$ ms (connected device) $C \sim \{4 \cdot 10^5, 2 \cdot 10^6\}$ for $B = \{1, 5\}$ MHz, respectively.

REFERENCES

- [1] G. Seco-Granados, J. A. López-Salcedo, D. Jiménez-Baños, G. López-Risueño, "Challenges in indoor Global Navigation Satellite Systems. Unveiling its core features in signal processing", IEEE Signal Processing Magazine, vol. 29, no. 2, pp. 108-131, 2012.
- [2] V. Lucas-Sabola, G. Seco-Granados, J. A. López-Salcedo, and J. A. García-Molina, "GNSS IoT positioning: from conventional sensors to a cloud-based solution," Inside GNSS, Vol. 3, no. May/June, pp. 53–62, 2018.
- [3] A. Hansen, S. Mackey, H. Wassag, and K. Van Dyke, "Complementary PNT technology demonstration", in Proc. of ION GNSS+, 2021.
- [4] M. Esanhoury, J. Koljonen, P. Valisuo, M. Emusrati, H. Kuusniemi, (2021) "Survey on recent advances in integrated GNSSs towards seamless navigation using multi-sensor fusion technology," in Proc of ION GNSS+, 2021.
- [5] G. Gao, and P. Enge, and L. Davis, et. al. "Global Navigation Satellite Systems: Report of a Joint Workshop of the National Academy of Engineering and the Chinese Academy of Engineering," National Academies Press, 2012.
- [6] J. A. del Peral-Rosado, and R. Raulefs, and J. A. López-Salcedo, and G. Seco-Granados, "Survey of cellular mobile radio localization methods: From 1G to 5G," IEEE Communications Surveys & Tutorials, vol. 20, no. 2, pp. 1124–1148, 2017.
- [7] T. Reid, A. Neish, T. Walter, and P. Enge, "Broadband LEO constellations for navigation," Navigation, vol. 65, no.2, pp. 205–220, 2018.
- [8] P. A. Iannucci, and T. E. Humphreys, "Economical Fused LEO GNSS," in Proceedings of the IEEE/ION PLANS, 2020.
- [9] M. Neinaavaie, Mohammad and J. Khalife, and Z. M. Kassas, "Exploiting Starlink signals for navigation: first results," in Proceedings of the ION GNSS+, 2021.
- [10] S. E. Kozhaya, and J. A. Haidar-Ahmad, and A. A. Abdallah, and Z. M. Kassas, and S. S. Saab, "Comparison of neural network architectures for simultaneous tracking and navigation with LEO satellites," in Proceedings of the ION GNSS+, 2021.
- [11] B. McLemore, and M. L. Psiaki, "GDOP of Navigation using Pseudorange and Doppler Shift from a LEO Constellation," in Proceedings of the ION GNSS+, 2021.
- [12] P. A. Iannucci and T. E. Humphreys, "First evaluation of Starlink signals for PNT: Don't give me the jitters!," in Proceedings of the ION GNSS+, 2021.
- [13] T. Reid, and B. Chan, and A. Goel, and K. Gunning, et. al., "Satellite navigation for the age of autonomy," in Proceedings of the IEEE/ION PLANS, 2020.
- [14] D. Egea-Roca, and J. A. López-Salcedo, and G. Seco-Granados, and E. Falletti, "Comparison of Several Signal Designs Based on Chirp Spread Spectrum (CSS) Modulation for a LEO PNT System," in Proceedings of the ION GNSS+, 2021
- [15] S. M. Kay, "Fundamentals of Statistical Signal Processing: Estimation Theory," Pearson education, vol. 1, 1993.
- [16] J. Cooley, and J. Tukey, "An algorithm for the machine calculation of complex Fourier series," in JSTOR: Mathematics of computation, vol. 19, no. 90, pp. 297–301, 1965.
- [17] A. Hoeller, R. Souza, O. López, et. al., "Analysis and performance optimization of LoRa networks with time and antenna diversity," in IEEE Acces, vol. 6, pp. 32820–32829, 2018.